

# A STATISTICAL ASSESSMENT OF CURRENT SEISMIC QUIESCENCE ALONG THE NORTH ANATOLIAN FAULT ZONE: EARTHQUAKE PRE-CURSORS

Serkan ÖZTÜRK

Gümüşhane University, Department of Geophysics, TR-29100, Gümüşhane, Turkey;  
serkanozturk@gumushane.edu.tr

## KEYWORDS

precursory seismic quiescence  
North Anatolian Fault Zone  
seismicity rate changes  
seismic hazard  
decluster

## ABSTRACT

The variations of the current seismicity rate on the North Anatolian Fault Zone in the beginning of 2009 have been analyzed based on the phenomenon of precursory seismic sequence before crustal main shocks. For this purpose, a statistical assessment is made to detect the seismic quiescence situation by using the standard normal deviate Z-value. Eight seismic quiescence regions are observed and quiescence anomalies in these regions have been observed since the beginning of 2005. On the Marmara part of the North Anatolian Fault Zone, four quiescence areas have been found on Silivri, in the Black Sea, around Izmit region and Çanakkale, Saros Gulf. On the Anatolian part of the North Anatolian Fault Zone, two quiescence areas have been observed on the Düzce fault and around the city of Amasya. Other anomalies have been observed around Erzincan, Elazığ and Bingöl regions on the eastern part of the North Anatolian Fault Zone.

Due to the occurrences of the last strong earthquakes " $M_w = 6.0$  - Elazığ earthquake, 2010 March 08;  $M_w = 5.2$  - Çanakkale (Saros Gulf) earthquake, 2010 November 03;  $M_w = 5.5$  - Erzincan earthquake, 2011 September 22 and  $M_w = 5.1$  - Marmara Ereğlisi (Tekirdağ) earthquake, 2012 June 07", other seismic quiescence regions may contribute to the forecasting of impending main shocks. Spatial and temporal estimates of the future seismic hazard of the North Anatolian Fault Zone are provided based on the results.

## 1. INTRODUCTION

In recent years, a number of studies have been made on the variation of seismicity before the occurrence of large earthquakes, including the phenomenon of precursory quiescence, as important tools for understanding seismo-tectonic processes (Murru et al., 1999). Though precursory seismic anomalies are important, they are controversial subjects. Among most of the reported precursory anomalies, seismic quiescence is defined as a significant decrease of the mean seismicity compared to the preceding background seismicity (Wu and Chiao, 2006). Several papers reported that precursory seismic quiescence occurred in and around focal areas several years before main shocks, e.g. Tokachi-Oki (Mogi, 1969), Tonga-Kermadec (Wyss et al., 1984), Morgan Hill (Habermann and Wyss, 1984), San Andreas (Wyss and Burford, 1987), Izu-Oshima (Wyss et al., 1996), Kurile (Katsumata and Kasahara, 1999), Colfiorito (Console et al., 2000), Kefalonia (Chouliaras and Stavrakakis, 2001).

Mogi (1969) proposed on the basis of visual inspection of seismicity maps that precursory seismic quiescence is the inner part of the doughnut pattern. In comparison with the preceding declustered background rate within all or a major part of the source volume, seismic quiescence is defined as a significant decrease in mean seismicity rate (Wyss and Martirosyan, 1998). The decrease in rate, which may last between one and several years, must precede and lead up to the main shock time, or may be separated from it by a relative

short period of an increased seismic activity rate (Murru et al., 1999). It is still not well established if the time dependence of the precursory quiescence on the expected main shock magnitude and the quiescence dimensions are in accordance with those of the source volume of the likely main shock. This may also be a function of the tectonic environment. Therefore, it is difficult to ascertain what characteristics of quiescence to expect, and it is not certain whether or not the quiescence occurs in all possible tectonic settings.

Considering the temporal and spatial properties of the most important seismic activity variations, seismic quiescence has provided additional insight into the problem of finding precursory anomalies related to the crustal main shock. From this point of view, the main goal of this work is to put forward statistical records concerning the intermediate-term earthquake prediction along the North Anatolian Fault Zone (NAFZ), by making a statistical analysis to detect the changes in the seismic activity in the beginning of 2009. For this purpose, the gridding method of Wiemer and Wyss (1994) and the ZMAP software (Wiemer, 2001) are used to map the precursory changes in the seismic activity along the NAFZ. Such studies show the recent seismic quiescence situation before several intermediate crustal events which have taken place in different parts of the world. Therefore, this analysis can give an important aspect to earthquake forecast research, and also allows to make a statistical assessment in detecting fu-

ture episodes of quiescence in real time at the NAFZ.

## 2. DATA ANALYSIS

### 2.1 DATA PREPARATION AND SEISMIC SOURCE ZONES

A part of the database used in this study is taken from Öztürk (2009), who developed some relationships between different magnitude scales ( $m_b$ -body wave magnitude,  $M_s$ -surface wave magnitude,  $M_L$ -local magnitude, and  $M_D$ -duration magnitude) to prepare a homogenous and complete earthquake catalogue from different data sets. For this purpose, Öztürk (2009) used the catalogue data from the website of the International Seismological Centre (ISC) during the period 1970 to 1973, and Bogazici University, Kandilli Observatory and Research Institute (KOERI), TURKNET, Incorporated Research Institutions for Seismology (IRIS) and TUBITAK from 1974 to 2005. Öztürk (2009) prepared a homogenous and complete instrumental data catalogue for  $M_D$  magnitude using these relationships. This catalogue for the duration magnitude includes 73,530 earthquakes whose magnitudes are equal to or are larger than 1.4, which occurred in Turkey between 1970 and 2005. Since Öztürk (2009) used the empirical relations to get a homogenous catalogue from 1970 to 2005, this magnitude level ( $M_D > 1.4$ ) is obtained. The KOERI catalogue is also used between 2006 and

2009. The Seismological Observatory of KOERI, computed the size of all earthquakes with  $M_D$  (in general  $M_D > 3.0$ ), which provides real time data with the modern on-line and dial-up seismic stations in Turkey. In general, KOERI gives  $M_L$  magnitude for the local earthquakes with missing  $M_D$  magnitudes. In the situation that  $M_D$  is unknown in the KOERI catalogue between 2006 and 2009,  $M_D$  magnitudes were calculated using the  $M_D$ - $M_L$  relationships (Table 1) from Öztürk (2009) and 12,068 earthquakes were obtained for this time interval in and around Turkey. The same relationships for  $M_D$ - $M_L$  scales are also given in detailed in Bayrak et al. (2009).

The bounds of the region analyzed in this study are provided from Öztürk (2009), who divided Turkey into different 24 source regions, and made a detailed zonation considering different previous zonation studies for modeling of seismic hazard in Turkey. Öztürk (2009) plotted the existing tectonic structure with the epicenter distribution of earthquakes, and the solution of focal mechanism given by TUBITAK for the great earthquakes occurred in Turkey between 1977 and 2002. Thus, a part of these seismic source zones is considered as the study region. The North Anatolian Fault Zone (regions 20, 21 and 24 in Öztürk, 2009) is selected as the area of investigation in this study. According to Öztürk (2009), region 20 (region 1 in this study) covers the Marmara part in the North Anatolian Fault Zone (MNAFZ), region 21 (region 2

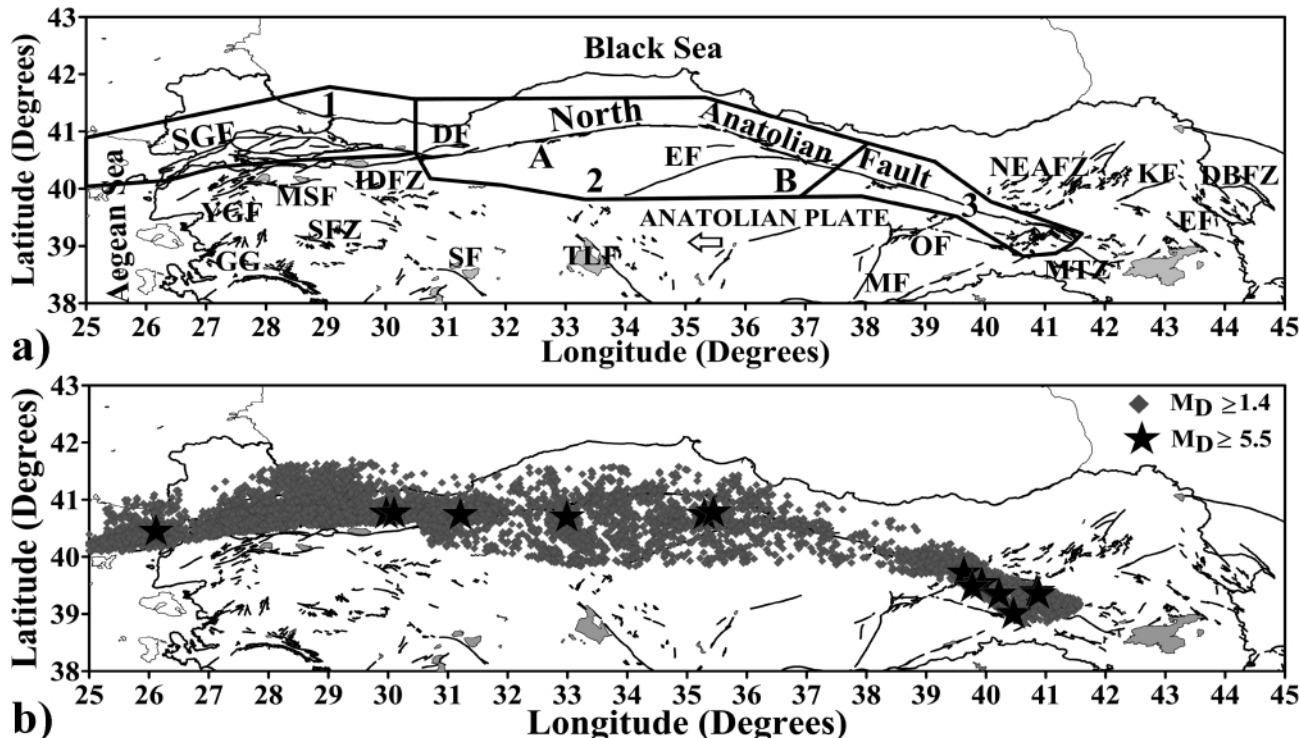


**FIGURE 1:** a) Active fault systems and seismic source zones in the North Anatolian Fault Zone. All tectonics were modified from Şaroğlu et al. (1992) while the seismic regions from Öztürk (2009). Several major faults are shown on the map. (1: Marmara part of the North Anatolian Fault Zone, 2: Anatolian part of the North Anatolian Fault Zone, 3: Eastern part of the North Anatolian Fault Zone, A: the Ismetpaşa segment, B: Erbaa city of Tokat province, IS: Ismetpaşa segment, EF: Erçis Fault, DBFZ: Doğu Beyazıt Fault Zone, NEAFZ: North East Anatolian Fault Zone, MTZ: Mus Thrust Zone, KF: Kagızman Fault, SF: Sultandagı Fault, SFZ: Simav Fault Zone, SGE: Saros-Gazikoy Fault, IDFZ: Inonu-Dodurga Fault Zone, MF: Malatya Fault, YGF: Yenice-Gonen Fault, MSF: Manyas Fault, GG: Gediz Graben, DF: Duzce Fault, TLF: Tuz Lake Fault, OF: Ovacık Fault, EF: Ezinepazarı Fault). b) Seismicity map of the North Anatolian Fault Zone for all earthquakes with  $M_D \geq 1.4$  and depth  $< 70$  km between February 1970 and December 2008. Stars indicate the principal main shocks with  $M_D \geq 5.5$ .

Region Number	Earthquakes Number	Calculated relationships	Correlation Coefficient (r)
1	20	$M_D = 0.881(\pm 0.138) * M_L + 0.596(\pm 0.286)$	0.820
2	14	$M_D = 0.919(\pm 0.023) * M_L + 0.292(\pm 0.048)$	0.996
3	11	$M_D = 0.991(\pm 0.080) * M_L + 0.033(\pm 0.158)$	0.966
4	24	$M_D = 0.768(\pm 0.114) * M_L + 1.004(\pm 0.239)$	0.808
5	4	-	-
6	26	$M_D = 0.816(\pm 0.068) * M_L + 0.825(\pm 0.147)$	0.920
7	14	$M_D = 0.812(\pm 0.112) * M_L + 0.726(\pm 0.234)$	0.889
8	2	-	-
9	11	$M_D = 0.432(\pm 0.339) * M_L + 2.293(\pm 0.675)$	0.359
10	23	$M_D = 0.843(\pm 0.066) * M_L + 0.580(\pm 0.137)$	0.935
11	81	$M_D = 0.818(\pm 0.036) * M_L + 0.586(\pm 0.075)$	0.929
12	46	$M_D = 1.277(\pm 0.209) * M_L - 1.372(\pm 0.434)$	0.669
13	12	$M_D = 1.113(\pm 0.389) * M_L - 0.555(\pm 0.768)$	0.636
14	29	$M_D = 0.956(\pm 0.057) * M_L + 0.103(\pm 0.114)$	0.952
15	70	$M_D = 0.934(\pm 0.029) * M_L + 0.163(\pm 0.062)$	0.967
16	15	$M_D = 0.446(\pm 0.146) * M_L + 1.900(\pm 0.291)$	0.619
17	67	$M_D = 0.748(\pm 0.043) * M_L + 0.869(\pm 0.089)$	0.903
18	12	$M_D = 0.886(\pm 0.044) * M_L + 0.349(\pm 0.087)$	0.985
19	18	$M_D = 0.901(\pm 0.049) * M_L + 0.268(\pm 0.100)$	0.974
20	62	$M_D = 0.939(\pm 0.068) * M_L + 0.091(\pm 0.138)$	0.867
21	22	$M_D = 0.876(\pm 0.069) * M_L + 0.450(\pm 0.139)$	0.939
22	17	$M_D = 0.873(\pm 0.043) * M_L + 0.467(\pm 0.089)$	0.980
23	11	$M_D = 1.229(\pm 0.691) * M_L - 0.707(\pm 1.382)$	0.473
24	21	$M_D = 0.743(\pm 0.099) * M_L + 1.211(\pm 0.222)$	0.851

**TABLE 1:** Magnitude conversion relationships between  $M_D$  and  $M_L$  scales for 24 different source regions of Turkey. The values in the parentheses show the uncertainties (from Öztürk, 2009)

in this study) is the Anatolian part of the North Anatolian Fault Zone (ANAFZ), and region 24 (region 3 in this study) covers the eastern part of the North Anatolian Fault Zone (ENAFZ). The major tectonic structures of the region are adopted from Şaroğlu et al. (1992) and the zones based on Öztürk (2009) are shown in Figure 1a. Additionally, the Ismetpaşa segment (A) and Erbaa city of Tokat province (B) are located in Figure 1a. (For details on the relationships of MS with the other magnitude types and all seismic zonations see Bayrak et al., 2009). After the selection of the study region along the North Anatolian Fault Zone, the earthquake data in this region was prepared. In this stage, earthquakes between the time interval 2006 and 2009 for regions 1, 2 and 3 are selected from the whole

catalogue. There have been totally 1,900 events in these three regions between 2006 and 2009. The time interval considered for the present work is from 1970 to 2009.  $M_D$ -duration magnitude is used. Thus, the prepared data catalogue for regions 1, 2 and 3 consists of 16,295 earthquakes (depth < 70 km) with magnitudes greater than or equal to 1.4. Epicenter distributions of whole earthquakes ( $M_D \geq 1.4$ ) and the strong main shocks ( $M_D \geq 5.5$ ) in the study region are shown in Figure 1b. All details of  $M_D \geq 5.5$  earthquakes are also given in Table 2. Also, a surface ruptures map along the NAFZ with the location of large earthquakes given in Table 2 are shown in Figure 2.

## 2.2 MAGNITUDE COMPLETENESS ANALYSIS AND DECLUSTERING OF DATA

The change of magnitude completeness,  $M_c$ , as a function of time is determined for all sub-regions by using a moving time window approach in order to analyze the frequency-magnitude relationship and plot the seismic quiescence.  $M_c$  is estimated for samples of 30 events/window for the MNAFZ by using the earthquake catalogue containing all 9,498 earthquakes of  $M_D \geq 1.4$ , 75 events/window for the ANAFZ by using the earthquake catalogue containing all 4,363 earthquakes of  $M_D \geq 1.4$ , and 30 events/window for the ENAFZ by using the earthquake catalogue containing all 2,434 earthquakes of  $M_D \geq 2.0$ . Figure 3 shows the variations of  $M_c$  versus time for all parts of the NAFZ. In the MNAFZ,  $M_c$  value is rather large and varies from 3.5 to 4.0 between 1975 and 1980, while  $M_c$  decreases to about 2.3 and 2.5 between 1980 and 1985 (Figure 3a). Then, it decreases to about 2.7 in the beginning of 1987. However, there are two maximum values of 4.0 and

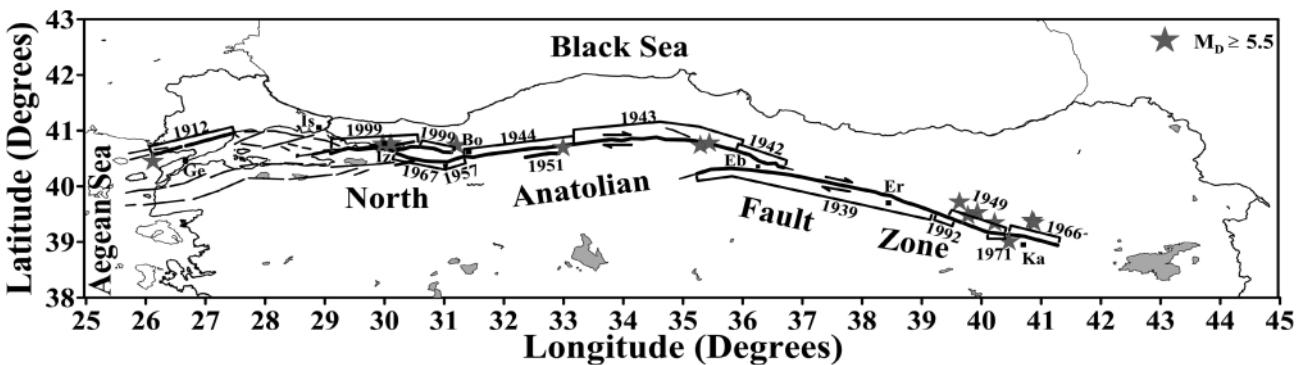


**FIGURE 2:** Historical surface ruptures with their dates along the North Anatolian Fault Zone and major earthquakes ( $M_D \geq 5.5$ ) given in Table 2. Place of surface ruptures were modified from Langridge et al. (2002). Ge: Gelibolu, Is: Istanbul, Iz: Izmit, Bo: Bolu, Eb: Erbaa, Er: Erzincan, Ka: Karliova.

and 3.3. These large values in region 1 are observed after the 1999 Izmit earthquake sequence. In the ANAFZ,  $M_c$  has a value between 3.0 and 3.5 until 1985 and around 3.0 between 1985 and 2000 (Fig. 3b). This  $M_c$  value is smaller than 3.0 after 2000, i.e. around 2.9. A large  $M_c$  value of 3.9 is observed in the 1999 Duzce aftershock sequence. In these two parts of the NAFZ, as stated in Wiemer and Katsumata (1999), some high  $M_c$  values may be higher in the early part of the aftershock sequence because the small shocks may not be located. In the ENAFZ,  $M_c$  value is rather large and exceeds 4.0 until 1995, and decreases from 4.0 to 3.1 between 1995 and 2003 (Fig. 3c). After 2003,  $M_c$  value varies between 2.8 and 3.1. Therefore, it can be inferred that  $M_c$  generally shows a non-stable value in the different parts of the NAFZ. However,  $M_c$  value varies between 2.7 and 2.9 in the NAFZ, and this result is consistent with the completeness analysis made by Huang et al. (2002).

There are 9,498 earthquakes with magnitudes greater than or equal to 1.4 in region 1. For this region,  $M_c$  value is 2.7 and the number of events exceeding this magnitude level is 6,242. Declustering algorithm subtracted 251 (about 4%) events and 37% of the events were totally removed from whole data set. Consequently, the number of earthquakes in the MNAFZ for Z-value calculations was reduced to 5,991. In region 2, there are 4,363 earthquakes with magnitudes larger than or equal to 1.4. For this region, the  $M_c$  value is 2.9 and the number of events exceeding this magnitude level is 3,048. Declustering algorithm subtracted 272 (about 9%) events and 36% of the events in total were removed from whole data set. Thus, the number of events in the ANAFZ for Z-value assessment was reduced to 2,776. There are 2,434 earthquakes with magnitudes greater than or equal to 2.0 in region 3. For this region,  $M_c$  value is 2.9 and the number of events exceeding this magnitude level is 1,847. Declustering algorithm subtracted 393 (about 21%) events and 40% of the events in total were removed from the entire data set. In conclusion, in the ANAFZ the number of events for Z-value analysis was reduced to 1,454. After

completing the declustering processes, a more reliable, homogeneous and robust seismicity data has been obtained for all sub-regions of the NAFZ.

### 3. TECTONICS AND SEISMICITY OF THE NORTH ANATOLIAN FAULT ZONE

The NAFZ is one of the best-known strike-slip faults in the world because of its remarkable seismic activity and extremely well developed surface expression (Bozkurt, 2001). The NAFZ is a very active structure, and according to geodesy it accom-

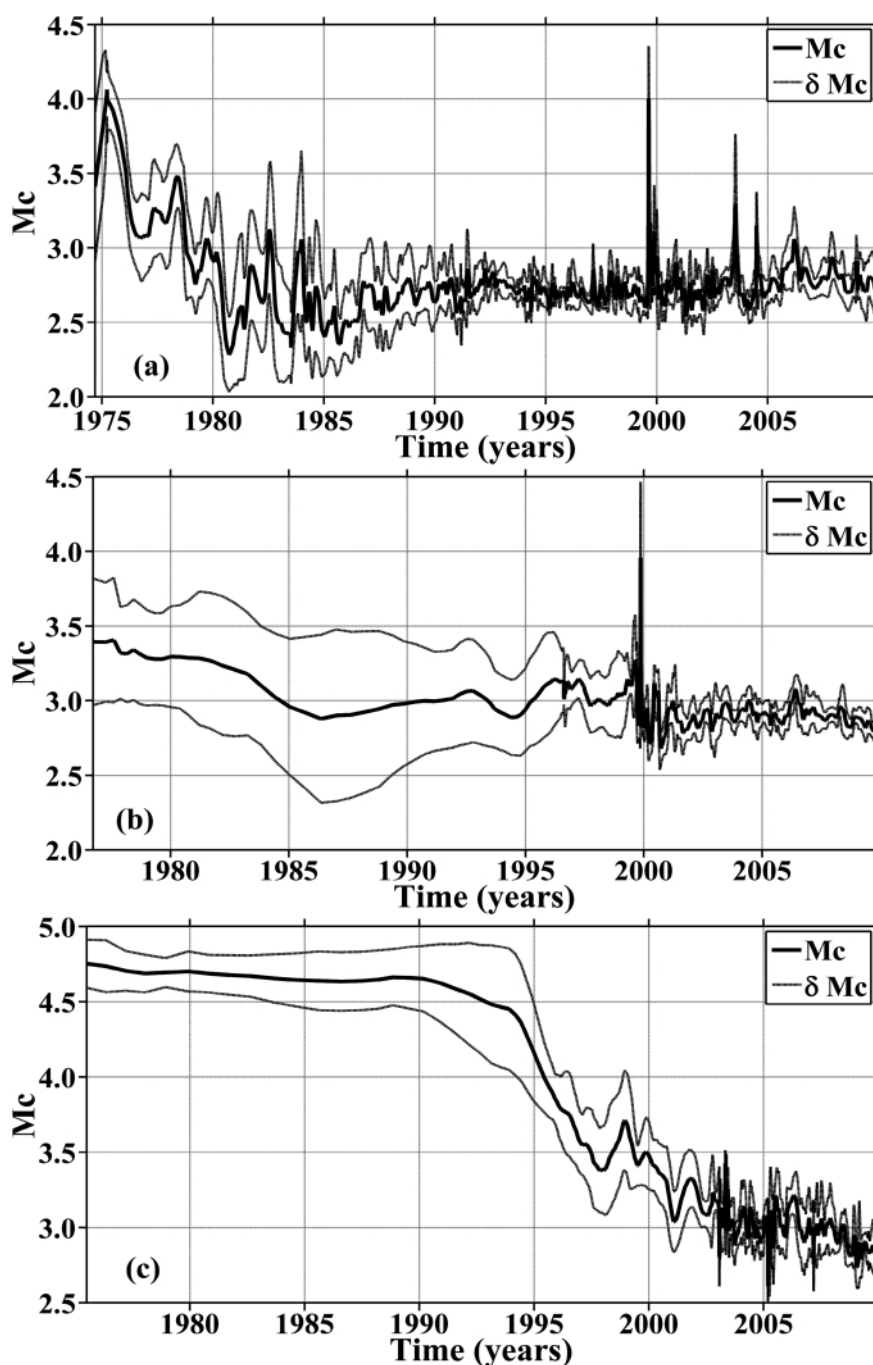


**FIGURE 3:** Magnitude completeness,  $M_c$ , as a function of time for (a) MNAFZ, (b) ANAFZ, and (c) ENAFZ. Standard deviation ( $\delta M_c$ ) of the completeness (dashed lines) is also given.  $M_c$  is calculated for overlapping samples, each containing 30 events for MNAFZ, 75 events for ANAFZ and 30 events for ENAFZ.

Year	Month	Day	Origin Time	Longitude	Latitude	Depth (km)	Magnitude ( $M_D$ )	Region
1975	03	27	05:15:08	26.12	40.45	15.0	5.7	1
1999	08	17	00:01:37	29.97	40.76	18.0	6.7	1
1999	09	13	11:55:28	30.10	40.77	19.0	5.8	1
1996	08	14	01:55:03	35.29	40.74	17.0	5.6	2
1997	03	08	23:01:58	35.44	40.78	5.0	6.0	2
1999	11	12	16:57:21	31.21	40.74	25.0	6.5	2
2000	06	06	02:41:49	32.99	40.70	5.0	5.6	2
1992	03	13	17:18:39	39.63	39.72	23.0	6.5	3
1992	03	15	16:16:25	39.93	39.53	29.0	6.0	3
1995	12	05	18:49:32	40.22	39.35	33.0	5.6	3
2003	01	27	05:26:08	39.77	39.48	5.0	6.1	3
2003	05	01	00:27:04	40.46	39.01	5.0	6.2	3
2005	03	12	07:36:09	40.85	39.39	4.0	5.6	3
2005	03	14	01:55:55	40.88	39.35	5.0	5.9	3

**TABLE 2:** General information of earthquakes occurred in study region with magnitude  $M_p \geq 5.5$

modates 24-30 mm/yr of dextral motion (Reilinger et al., 1997). The NAFZ is an approximately 1,500 km-long, broadly arc-shaped, dextral strike-slip fault system that extends from eastern Turkey in the east to the north Aegean in the west. It is predominantly a single zone ranging from a few hundred meters to 40 km wide. Along much of its length, this fault zone consists of a few shorter subparallel fault strands that sometimes display an anastomosing pattern (Bozkurt, 2001). The NAFZ forms a typical triple-junction to the east, and joins with the sinistral East Anatolian Fault Zone (EAFZ) at Karlıova. The NAFZ does not terminate at the Karlıova triple junction but

continues towards south east. This section ruptured during two successive earthquakes on August 19 and 20, 1966 ( $M=6.8$  and  $M=6.2$ ), respectively (Ambraseys, 1988). During the past 60 years, the NAFZ has produced earthquakes along different sections in a system manner that is atypical of long faults. Beginning with the 1939 Erzincan earthquake ( $M=7.9$  to 8.0), which produced about 350 km of ground rupture, the NAFZ ruptured by nine moderate to large earthquakes ( $M>6.7$ ), and formed more than 1,000 km surface rupture along the fault. Most of the earthquakes occurred sequentially in a westward progression. These include

9 August 1912 Marmara ( $M=7.4$ ), 26 December 1939 Erzincan ( $M=7.9$  to 8.0), 20 December 1942 Erbaa-Niksar ( $M=7.1$ ), 26 November 1943 Tosya ( $M=7.6$ ), 1 February 1944 Bolu-Gerede ( $M=7.3$ ), 17 August 1949 Elmalıdere-Bingöl ( $M=7.1$ ), 13 August 1951 Kurşunlu-Çankırı ( $M=6.9$ ), 26 May 1957 Abant ( $M=7.0$ ), 22 July 1967 Mudurnu valley ( $M=7.1$ ), 22 May 1971 Bingöl ( $M=6.7$ ), 13 March 1992 Erzincan ( $M=6.8$ ), 17 August 1999 Izmit ( $M=7.4$ ), and 12 November 1999 Düzce earthquakes (Bozkurt, 2001).

#### 4. METHOD OF ANALYSIS

Temporal variations of the earthquake numbers and the related statistics are generally marked by aftershock activity. For the good-quality analysis of seismic activity variations, it is necessary to eliminate the dependent events from the catalogue. The earthquake catalogue is declustered using the Reasenberg (1985) algorithm in order to separate the dependent events from the independent ones. This cluster analysis algorithm “declusters” or decomposes a regional earthquake catalogue into main and secondary events (Arabasz and Hill, 1996). This algorithm removes all the dependent events from each cluster, and substitutes them with a unique event, equivalent in energy to that of the whole cluster.

In recent years, *ZMAP* has been used to investigate seismic quiescence phenomena (e.g. Murru et al., 1999; Console et al., 2000; Chouliaras and Stavrakakis, 2001; Wu and Chen, 2007; Polat et al., 2008; Gentili, 2010; Rudolf-Navaro et al., 2010; Wang et al., 2010; Kumazawa et al., 2010). The new release of *ZMAP* (version 6-freely available on the web page, [http://www.seismo.ethz.ch/prod/software/zmap/index\\_EN](http://www.seismo.ethz.ch/prod/software/zmap/index_EN)) includes most of the routines adapted for Matlab and used for statistical analyses.

One of the statistical methods frequently used for analyzing seismicity rate changes is the standard normal deviate *Z*-test (Wyss, 1986; Habermann, 1988; Wiemer and Wyss, 1994; Wu and Chiao, 2006). *ZMAP* produces a continuous image of seismicity rate changes in space and time by creating a grid of geo-

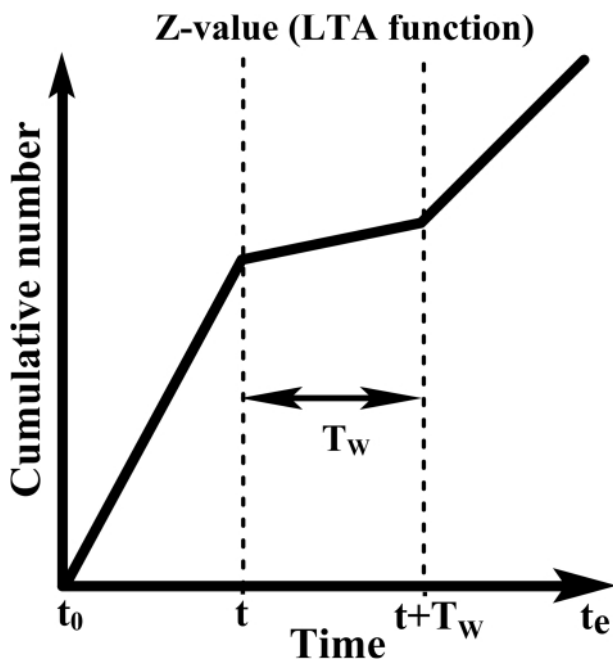


**FIGURE 4:** Schematic explanation of how to calculate *Z*-value. The *Z*-value is calculated for all times  $t$  between  $t_0$  and  $t_e$  to  $T_w$  and is statistically appropriate for estimating seismicity rate change in a time window  $T_w$  in contrast with background seismicity.  $T_w$  is the length of the time window in year and  $t$  is the “current time” ( $t_0 < t < t_e$ ).

graphical coordinates, and associating to each grid node a selected number of nearest events. The subset of events belonging to each grid node is sampled in short time windows (usually a few weeks), so that the average number of events occurred in a time period of several consecutive samples (foreground) can be compared with that of all the remaining samples (background). The ZMAP method is applied for imaging the areas exhibiting a seismic quiescence (for details see Wiemer and Wyss, 1994). In order to rank the importance of quiescence, the standard deviate Z-test is used, generating the LTA( $t$ ) (Long Term Average) function for the statistical evaluation of the confidence level in units of standard deviations (Wiemer and Wyss, 1994)

$$Z(t) = \frac{R_{all} - R_{wl}}{\sqrt{\frac{\sigma_{all}^2}{n_{all}} + \frac{\sigma_{wl}^2}{n_{wl}}}} \quad (1)$$

where  $R_{all}$  is the mean rate in the overall period including  $T_w$  (from  $t_0$  to  $t_0$ ),  $R_{wl}$  the mean rate in the considered time window (from  $t$  to  $t+T_w$ ),  $\sigma_{all}$  and  $\sigma_{wl}$  are the standard deviations in these periods, and  $n_{all}$  and  $n_{wl}$  the number of samples and  $t$  is the "current time" ( $t_0 < t < t_0$ ) (Katsumata and Kasahara, 1999). The Z-value, computed for all times  $t$  between  $t_0$  and  $t_0 - T_w$  (Figure 4), by the equation is statistically appropriate for estimating seismicity rate change in a time window  $T_w$  (also indicated as  $iwl$ ) in contrast with background seismicity. The Z-value calculated as a function of time, letting the foreground window slide along the time duration of catalogue, is called LTA( $t$ ). The shape of the LTA( $t$ ) function strongly depends on the choice of the length of the foreground window ( $iwl$ ). While the statistical robustness of the LTA( $t$ ) function increases with the size of  $iwl$ , its shape becomes increasingly smooth, if the  $iwl$  length exceeds the duration of the anomaly. Moreover, if one evaluates the statistical significance of an anomaly, it is not only necessary to decide the threshold level for the Z-value (in terms of standard deviations unit), but it is also necessary to decide the maximum time length allowed after the end of the anomaly, before the occurrence

of the main shock. The duration of quiescence is a significant parameter to be determined and its importance is maximized when  $T_w$  is equal to that value and for meaningful results it is demanded that they do not depend on the choice of  $T_w$ . Since it is not known how long quiescence may last, the window length was changed from 1.5 to 5.5 years, because this is in the range of reported seismic quiescence prior to crustal main shocks (Wyss, 1997a; 1997b).

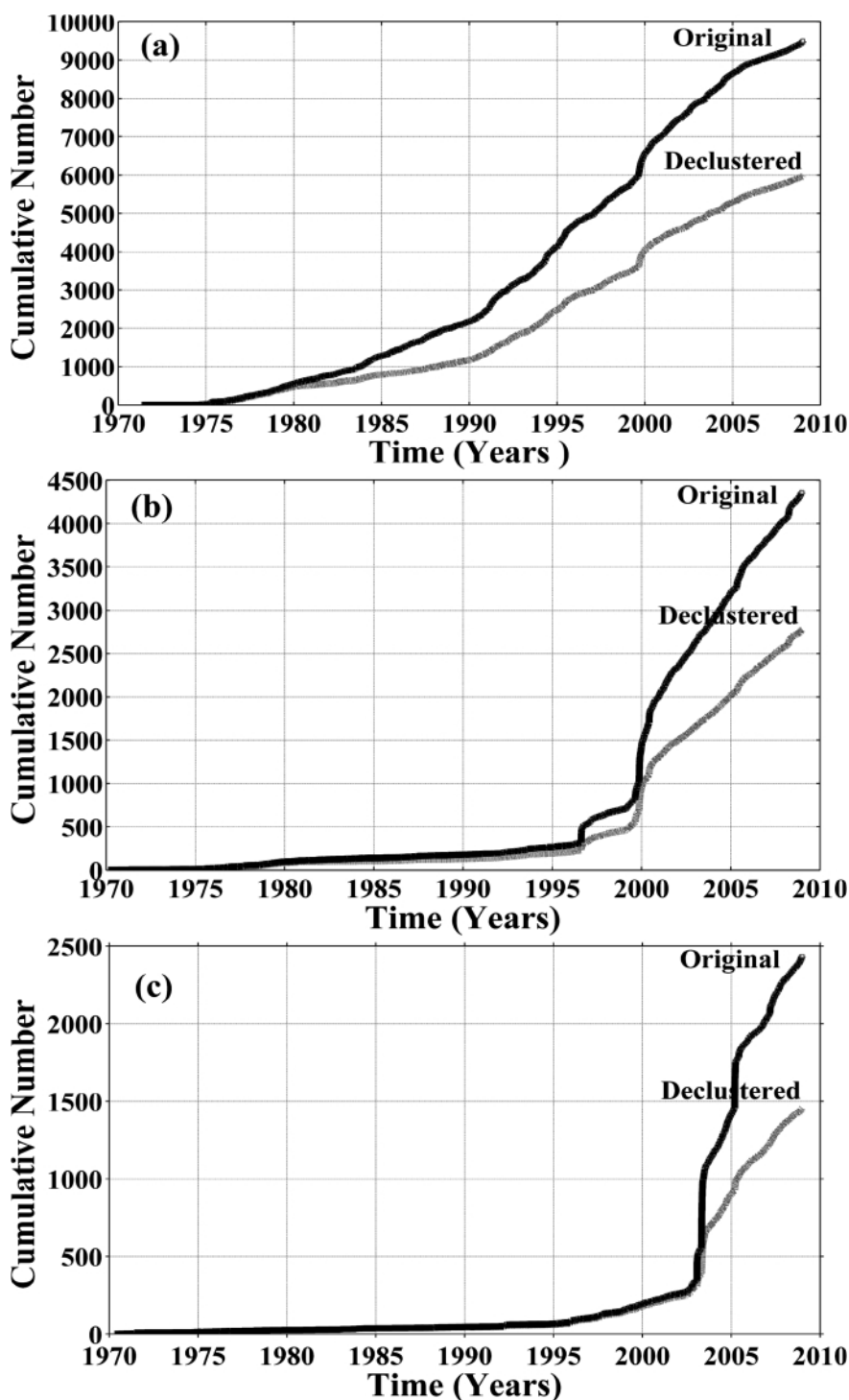


FIGURE 5: Plots of cumulative number of events versus time for original and declustered earthquake catalogues for all sub-regions of the North Anatolian Fault Zone: (a) for MNAFZ, (b) for ANAFZ and (c) for ENAFZ.

To establish the regional distribution of the seismic quiescence mentioned above, the Reasenberg (1985) method is applied to decluster the data. Details of the method are described, e.g., in Wiemer and Wyss (1994). Therefore, only a brief summary is provided in this study. The Z-maps based on the declustered catalogue represents a choice obtained after numerous tests, carried out trying different  $T_w$  values (indicated as  $iwl$  in the respective figures) such as 1.5, 2.5, 3.5, 4.5 and 5.5 years and different starting times for the foreground windows. Each Z-value is represented by a different color: the scale spans from the lowest Z-values, indicating no significant changes in seismicity rate, shown in black, and the highest ones (decrease in seismicity rate), shown in grey. Then, the

calculated Z-values are contoured and mapped.

### 5. RESULTS

Figure 5 shows the cumulative number of earthquakes against time in all regions for original catalogue and for declustered events (excluding dependent events from the original catalogue). For region 1, there is no significant seismic change of reporting as a function of time between 1970 and 1975 (Fig. 5a). As shown in the cumulative number of earthquakes as a function of time for regions 2 (Fig. 5b) and 3 (Fig. 5c), little change is observed in the seismic activity after 1970 until 1995 but further on, great changes are obvious in the studied area, especially after 2000. Because many stations have been

built in this area in recent years, especially after the great earthquakes in Izmit and Düzcein 1999, other observatories and mainly KOERI provides the real time data with the modern on-line and dial-up seismic stations in Turkey. Since this evaluation deals with the seismicity rate change and not energy or moment release, the magnitude of completeness of the catalogue used to detect the quiescence is an important parameter because this varies regionally depending on the seismic activity of the area under investigation and the detectability of the network.

The  $b$ -value in Gutenberg and Richter (1944) relationship is calculated by the maximum likelihood method using ZMAP software, because it yields a more robust estimate than the least-square regression method (Aki, 1965). Gutenberg-Richter (G-R) law describes the power-law of size distribution of earthquakes. Figure 6 shows the plots of cumulative number of the earthquakes versus the magnitude for all regions. The catalogue includes 9,498 earthquakes ( $M_b \geq 1.4$ ) for epicentral depths less than 70 km for region 1.  $M_c$  value is calculated as 2.7 and the  $b$ -value is calculated as  $1.13 \pm 0.01$  using this  $M_c$  value for region 1 (Fig. 6a). The catalogue includes 4,363 events ( $M_b \geq 1.4$ ) for epicentral depths less than 70 km for region 2.  $M_c$  value is computed as 2.9 and using this value the  $b$ -value is found as  $0.99 \pm 0.02$  for region 2 (Fig. 6b). For region 3, the catalogue includes 2,434 events ( $M_b \geq 2.0$ ) for epicentral depths less

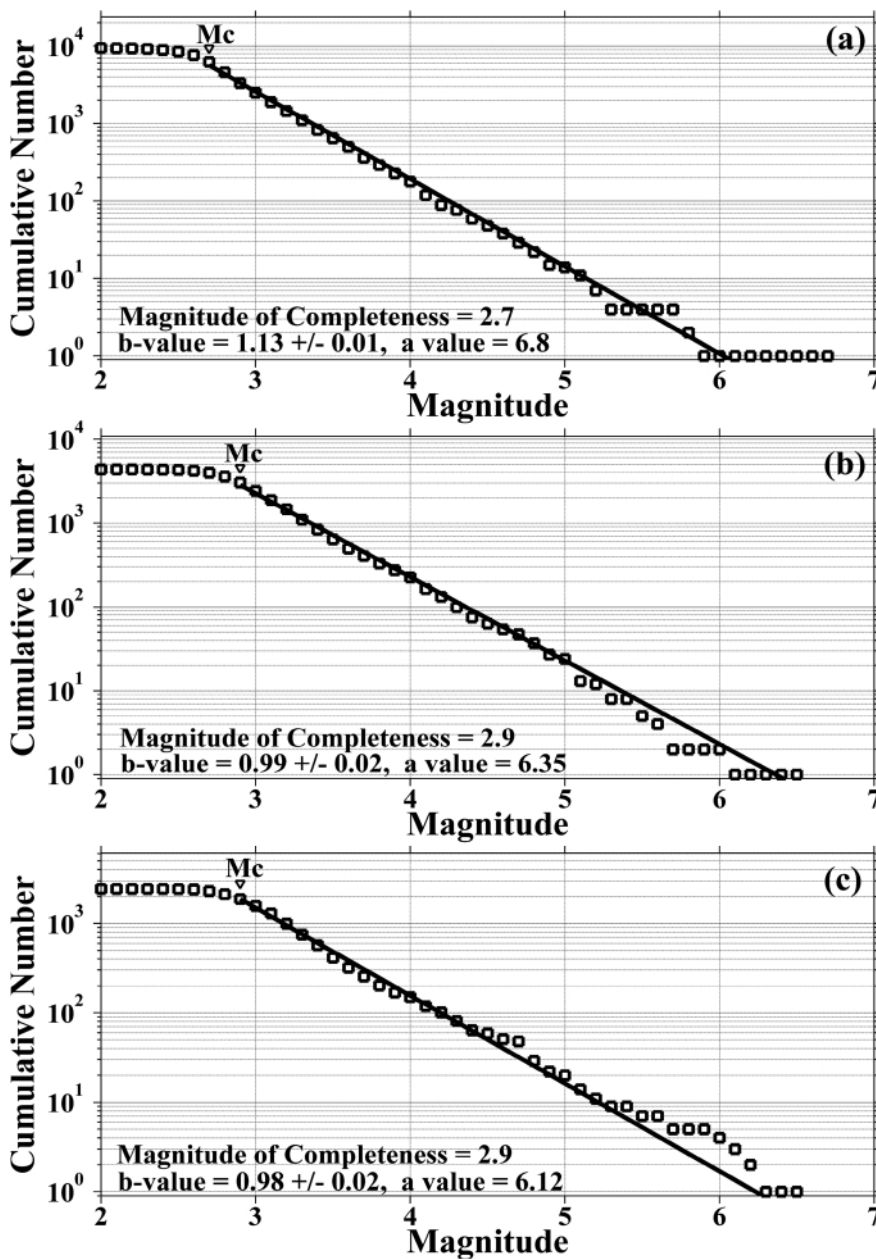


**FIGURE 6:** Magnitude-frequency distribution for all original catalogues between 1970 and 2009 for all sub-regions of the North Anatolian Fault Zone. The  $b$ -value and its standard deviation, as well as the  $a$ -value in the Gutenberg-Richter relation are given on the plots (a) for MNAFZ, (b) for ANAFZ and (c) for ENAFZ.

than 70 km.  $M_c$  value is taken as 2.9 and using this completeness value the  $b$ -value is calculated as  $0.98 \pm 0.02$  for region 3 (Fig. 6c). For all regions, the  $b$ -value and its standard deviation is determined with the maximum likelihood method, as well as the  $a$ -value of the Gutenberg-Richter relation. The tectonic earthquakes are characterized by the  $b$ -value from 0.5 to 1.5 and are more frequently around 1.0. It is clearly seen that the earthquake catalogue matches the general property of events such that magnitude-frequency distribution of the earthquakes is well represented by the Gutenberg-Richter law with a  $b$ -value typically close to 1.0 (Reasenberg and Jones, 1989).

The areas under analysis were divided into rectangular cells spacing  $0.02^\circ$  in longitude and latitude because this is related to the accuracy of epicentral determinations of the catalogue, and it also provides a dense coverage in space. The nearest earthquakes  $N=50$  for regions 1 and 2 and  $N=25$  for region 3 at each node are considered after some preliminary tests, and the seismicity rate changes are searched within a maximum radius changes by a moving time window  $T_w$ , stepping forward through the time series by a sampling interval as described by Wiemer and Wyss (1994). The shape of the LTA function strongly depends on the choice of the length of the foreground window ( $iwl$ ). While the statistical robustness of the LTA function increases with the size of  $iwl$ , its shape becomes more and smoother, if the  $iwl$  length exceeds the duration of the anomaly. The time window, equal to 5.5 years is used as the window length because the quiescence regions are better visible for a window of 5.5 years. Because the quiescence anomalies found in Figures 7, 9 and 11 are the best revealed at the epicentral areas for  $T_w$  equal to 5.5 years, this time window length is used in order to image the geographical distribution of the seismicity rate changes. The  $N$  and  $T_w$  values are usually selected accordingly to enhance the quiescence signal, and this choice does not influence the results in any way. For each grid point the earthquake population is binned into many binning spans of 28 days for all regions in order to have a continuous and dense coverage in time. Thus, spatial distributions of  $Z$ -values are presented for the beginning of 2009. All details for input parameters, some information about the study regions and the earthquake catalogues are given in Table 3.

As shown by the  $Z$ -value distribution along the MNAFZ (Fig. 7), four areas (A, B, C and D) exhibit significant seismic quiescence. Cumulative number plots of events and the correspondent LTA( $t$ ) function in a circular area including these regions are given in Figures 8a to 8d, respectively (Fig. 8a plotted for a circle of 13.77 km radius centered at region A with  $Z_{max}=6.5$ , Fig. 8b for a circle of 51.24 km radius centered at region B with  $Z_{max}=6.8$ , Fig. 8c for a circle of 10.54 km radius centered at region C with  $Z_{max}=6.0$  and Fig. 8d for

a circle of 16.03 km radius centered at region D with  $Z_{max}=4.4$ ) Seismic quiescence changes started in the beginning of 2005 in these four anomaly regions.

Two areas (E and F) exhibit seismic quiescence anomaly based on  $Z$ -value distribution along the ANAFZ (Fig. 9). Cumulative number plots for anomaly areas covering the regions E and F (Fig. 10a shows the cumulative earthquake number against time for a circle of 15.91 km radius centered at region E with  $Z_{max}=3.3$ , and Fig. 10b the cumulative earthquake number against time for a circle of 13.13 km radius centered at region F with  $Z_{max}=2.4$ ) shows the onset of seismic quiescence at nearly the beginning of 2005 in these two quiescence areas.

Figure 11 shows the  $Z$ -value distribution in the ENAFZ with two areas (G and H) exhibiting seismic quiescence anomaly. Cumulative number plots for anomalies areas covering the regions G and H are given in Figures 12a and 12b, respectively. Figure 12a shows the cumulative earthquake number against time for a circle of 9.70 km radius centered at region G with  $Z_{max}=2.3$  and Figure 12b shows the cumulative earthquake number against time for a circle of 12.88 km radius centered at region H with  $Z_{max}=2.6$ . The onset of seismic quiescence is again observed in the beginning of 2005.

For all cumulative number figures, the length of time window is determined by adding  $T_w$  value in years to the chosen time as the beginning of the time cut (indicated in the corresponding figures). So, all figures present the  $Z$ -value variations for the same time for all regions, the beginning of 2009. In the  $Z$ -value maps for all part of the NAFZ, eight areas exhibit significant seismic quiescence. In the MNAFZ, the first anomaly is found centered at  $41.08^\circ\text{N}-28.58^\circ\text{E}$  (region A, around Silivri) and the second one is found centered at  $41.47^\circ\text{N}-29.51^\circ\text{E}$  (region B, in the Black Sea). The third quiescence anomaly is observed centered at  $40.69^\circ\text{N}-29.78^\circ\text{E}$  (region C, including Izmit) and the fourth one is observed centered at  $40.26^\circ\text{N}-26.46^\circ\text{E}$  (region D, around Çanakkale, Saros Gulf). For all areas in the MNAFZ, anomalies in duration have been seen since the beginning of 2005 as shown in Figures 8a to 8d. In the ANAFZ, the first anomaly is found centered at  $40.59^\circ\text{N}-31.03^\circ\text{E}$  (region E, including Düzce fault) and the second quiescence area is found centered at  $40.86^\circ\text{N}-35.30^\circ\text{E}$  (region F,

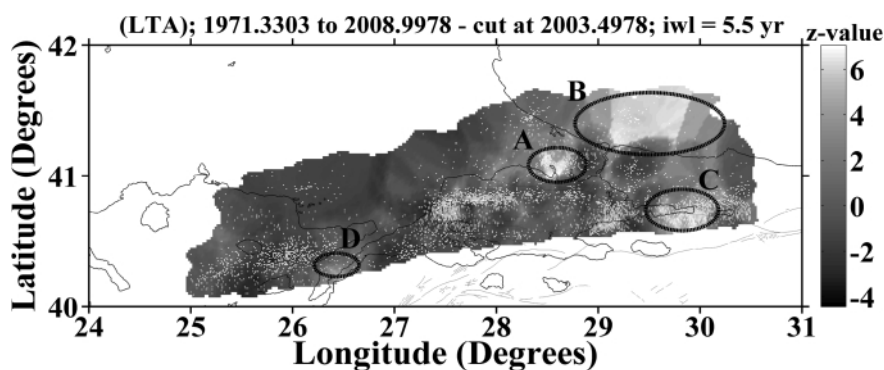


**FIGURE 7:** Spatial variability of  $Z$ -value for the Marmara part of the North Anatolian Fault Zone in the beginning of 2009 with  $T_w$  ( $iwl$ )=5.5 years. Calculations are made by using the declustered earthquakes with  $M_p \geq 2.7$  for this region.

around Amasya). While the anomalies in duration in the first quiescence for region E have been seen since the beginning of 2005, the second quiescence anomaly in region F has started in the beginning of 2003 as shown in Figures 10a to 10b. In the ENAFZ, the first anomaly is found centered at 39.48°N-39.74°E (region G, around Erzincan) and the second anomaly is found centered at 39.06°N-40.50°E (region H, including Elziğ and Bingöl). For the ENAFZ, the anomalies in duration have been seen since the beginning of 2005 as seen in Figures 12a to 12b.

There are some small quiescence areas in the ANAFZ aside from these eight significant areas mentioned above. One of them is observed on the Ismetpaşa segment (arrow 1 in Fig. 9) and the others (arrows 2 and 3 in Fig. 9) in the southwest of this segment. However, since these small quiescence areas are unclear, it is considered they are not as significant as the other eight quiescence regions. Also, since there are fewer earthquakes in some edges (especially in Bleak Sea region, or the other regions that have no fault system), these values in the abovementioned regions can be interpreted as artificial results from contouring and interpolations. Joswing (2001) stated that characterizing the null hypothesis must be made before the interpretation of seismic quiescence maps. For earthquake predictions, this means the fraction of success which is achieved by pure chance. Such kind of quiescence maps do not issue any alert but should help to relate quiescence spots to pending earthquakes. Thus, the null hypothesis describes how many quiescence anomalies would precede

a real event, even if the distribution is completely random. Also, in some regions the small scale quiescence anomalies can be interpreted as false alarms exceeding in significance the precursors. This randomness could be derived from the given catalogue by arbitrarily altering the event times, but keeping their locations for the spatial clustering (Joswing, 2001). Consequently, such kind of heterogeneous reporting as a function of time can generate false alarms and impede reliable measurement of natural seismicity rate changes.

## 6. DISCUSSIONS

In order to present the temporal and spatial implications of earthquake hazard in different parts of Turkey, especially in the North Anatolian Fault Zone, in recent years, many authors have used many different methods and made a large number of statistical analyses (e.g., Kutoglu and Akcin, 2006; Bektas et al., 2007; Kutoglu et al., 2008; Öztürk et al., 2008; Turk and Gumusay, 2008).

Kutoglu and Akcin (2006) and Kutoglu et al. (2008) determined the surface creep on the Ismetpaşa segment of the NAFZ after the Izmit and Duzce earthquakes in 1999 occurred in the near west of the Ismetpaşa segment based on the periodical observations of an old trilateration network. Their evaluation of the observations revealed a creep of 0.78 cm/year for the period 1992-2002 and this new observation campaign of the Ismetpaşa geodetic network shows that the Ismetpaşa segment has ceased the slowing trend and started to gain speed. They interpreted that the Ismetpaşa segment of the NAFZ is

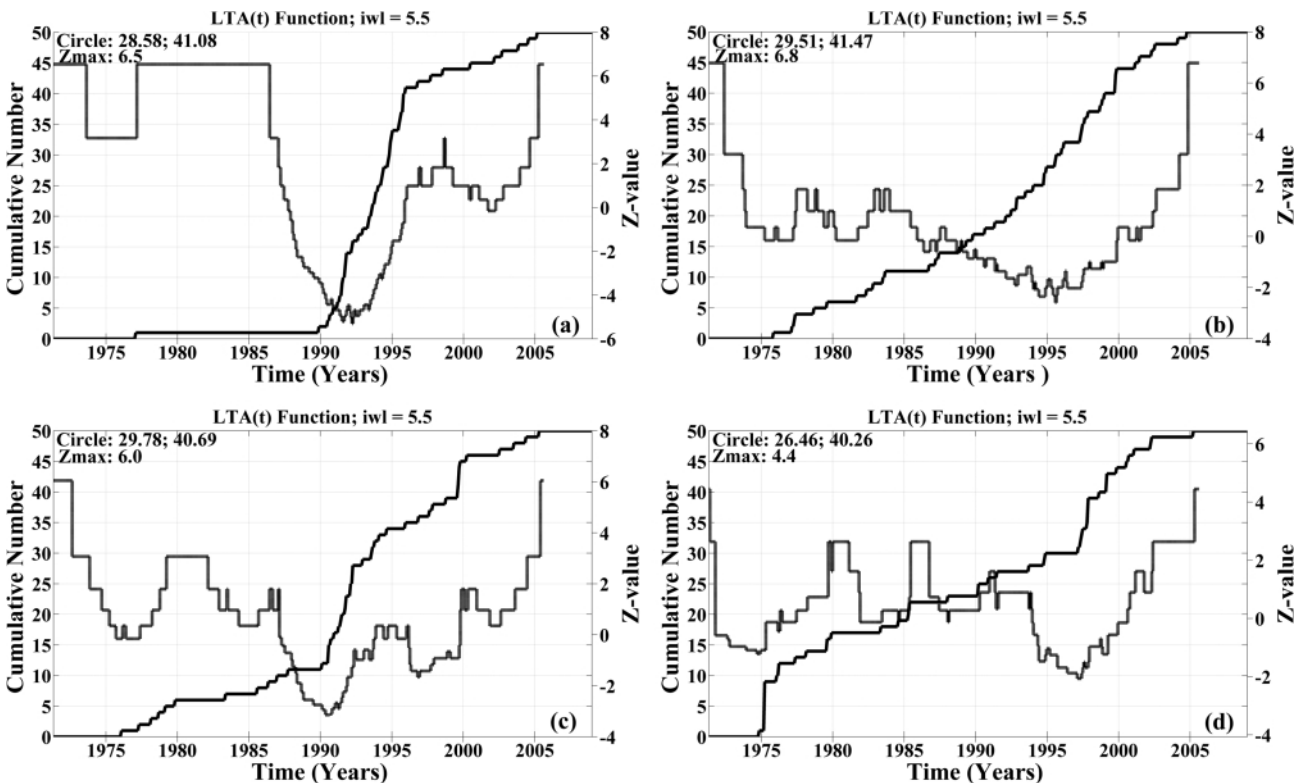


FIGURE 8: Cumulative number and Z-value plots versus time for the anomaly areas detected in in the Marmara part of North Anatolian Fault Zone in Figure 7 for (a) region A, (b) region B, (c) region C and (d) region D.

under an increasing earthquake risk. Although the quiescence observed in this analyze on the Ismetpaşa segment (region A in Fig. 1a) is in a small region and is not very clear, this can be interpreted as an earthquake risk for this segment.

Turk and Gumusay (2008) designed a disaster information system infrastructure and implemented it to take measures against natural hazards, especially earthquake on the NAFZ prior to natural disasters. They tested the system on the NAFZ in Erbaa city of Tokat province of Turkey. The created system performs processes such as determination of the risk for the city, taking the measures for probable dangerous earthquakes. They concluded that Erbaa is one of the riskiest cities on the NAFZ. However, any quiescence anomalies are not observed in the Erbaa region (region B in Fig. 1a) in this analysis.

A quantitative appraisal of earthquake hazard parameters using Gumbel's first asymptotic distribution for different regions in and around Turkey was made by Öztürk et al. (2008). They prepared a uniform catalogue of  $M_s$  between 1900 and 2005. They calculated the mean return periods, the most probable magnitude and the probability of earthquake occurrence for a given magnitude in a time period of 10, 25, 50 and 100 years for different 24 regions in and around Turkey. Öztürk et al. (2008) found that the mean return period value for  $M_s \geq 5.5$  in region 20 covering the MNAFZ is equal to  $11.22 \pm 0.39$  years. In addition, the probability of occurrence is equal to 60 percent in the next 10 years for the earthquakes with this magnitude level in region 1 according to their study. The last event of magnitude  $M_b \geq 5.5$  occurred in 1999 (see Table 2) in the MNAFZ. Thus, the next time with a probability of 60% for that size of earthquakes can be considered as 2010 in the MNAFZ. For the ANAFZ, the mean return period for  $M_s \geq 5.5$  is calculated as  $6.24 \pm 1.52$  years and the probability of occurrence for the earthquakes in this magnitude range is computed as 80 percent for the next 10 years by Öztürk et al. (2008). The last event with magnitude  $M_b \geq 5.5$  occurred in 2000 in the ANAFZ. The next time with a probability of 80% for that size of earthquakes can be considered as 2006 in the

	Region 1	Region 2	Region 3
<b>Study region</b>	40-42°K 24-31°D	39-42°K 30-38°D	38-41°K 37-42°D
<b>Time interval</b>	1 May 1971 31 December 2008	11 February 1970 31 December 2008	21 April 1970 27 December 2008
<b>Time length (year)</b>	37.67	38.88	35.64
<b>Completeness magnitude</b>	$M_D \geq 2.7$	$M_D \geq 2.9$	$M_D \geq 2.9$
<b>Depth interval (km)</b>	1-63	1-70	1-70
<b>Earthquake numbers (whole catalog)</b>	9498	4363	2434
<b>Earthquake numbers (declustered catalog)</b>	5991	2776	1454
<b>Grid space</b>	0.02°x0.02°	0.02°x0.02°	0.02°x0.02°
<b>Nearest earthquakes (N)</b>	50	50	25
<b>Window length (year)</b>	5.5	5.5	5.5
<b>Time steps (day)</b>	28	28	28

TABLE 3: Input parameters used in ZMAP computer program and some properties of study regions.

ANAFZ. Thus, the return periods have been exceeded for this size of main shocks. However, the mean return period for  $M_s \geq 6.0$  is found as  $11.48 \pm 1.59$  years in the ANAFZ by Öztürk et al. (2008). Also, the probability of occurrence for this magnitude size is computed as 58%. Considering this magnitude range, the next time with a probability of 58% for  $M_b \geq 6.0$  can be considered as 2011 in the ANAFZ. In the ENAFZ, the mean return period for the earthquakes with  $M_s \geq 5.5$  is indicated by Öztürk et al. (2008) with a value of  $7.50 \pm 0.09$  years, and they estimated the probability of occurrence for the earthquakes having the same size as 74% in the next 10 years. The last event with magnitude  $M_b \geq 5.5$  occurred in 2005 in the ENAFZ. So, the next time with a probability of 58% for this magnitude

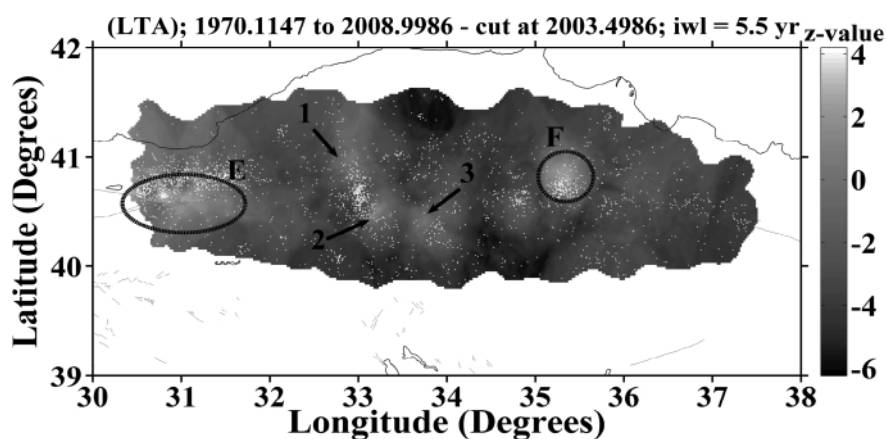


FIGURE 9: Spatial variability of Z-value for the Anatolian part of the North Anatolian Fault Zone in the beginning of 2009 with  $T_w$  (iwl)=5.5 years. Calculations are made by using the declustered earthquakes with  $M_b \geq 2.9$  for this region.

level can be considered as 2012 in the ENAFZ.

As shown in Figure 2, the Anatolian Block moves the west and south along the NAFZ and the EAFZ. The earthquakes migrate westward since 1939, and the surface ruptures caused by the earthquakes consist of many segments along the NAFZ (Langridge et al., 2002). While the 1912 Marmara earthquake produced 90 km surface rupture, the 1939 Erzincan earthquake produced 350 km surface rupture, the 1942 Erbaan-Niksar (Tokat) earthquake 50 km, the 1943 Tosya earthquake 265 km, the 1944 Gerede (Bolu) earthquake 180 km, the 1949 Elmalidere (Bingöl) earthquake 76 km, the 1951 Kurşunlu (Çankırı) earthquake 49 km, the 1957 Abant (Bolu) 40 km, the 1966 Varto-Üstükran (Muş) earthquake 38 km, the 1967 Mudurnu (Bolu) earthquake 80 km, the 1971 Bingöl earthquake 38 km, the 1992 Erzincan earthquake 30 km, the 1999 Izmit earthquake 200 km and the 1999 Düzce earthquake 41 km. Since the study period covers the time interval between 1970 and 2009, the epicenters of earthquakes before 1970 were not included. As discussed above, many authors used different statistical methods to characterize the seismic hazard or risk for different parts of the NAFZ. As seen in Z-value maps for all parts of the fault zone, seismic quiescence anomalies are

generally observed in and around historical main shock regions. In the MNAFZ (region 1), two seismic quiescence anomalies (in region C and D) are observed around the rupture areas of 1912 and 1999. As stated above, the anomaly observed in Black Sea (region B), or the other regions that have no fault system, can be interpreted as false alarms. In the ANAFZ (region 2), while one of the quiescence areas (region E) is found around 1999 Düzce earthquake region, the second quiescence area (region F) is observed around 1996 and 1997 earthquake regions. In the ENAFZ, two seismic quiescence regions are related with the rupture areas between 1949 and 1992. Thus, it can be said that the connection of past earthquakes with seismic quiescence for predicting future earthquakes can help a better interpretation.

Based on these previous studies, it seems now possible to predict some, if not all, of the major earthquakes several years prior to the main shock by monitoring the seismicity rate. Unfortunately, almost all precursory seismicity rate changes were identified not before but after the main shock. The present work detects precursory seismicity anomalies and identifies them as possible precursors to a main shock before the occurrence of the main events. This provides an experiment in intermediate-term earthquake prediction in the NAFZ. The conclusions in our study are in accordance with the results in the studies for the NAFZ by the authors mentioned above. Also, four strong earthquakes have occurred in these areas in recent years. The first of them was 08 March, 2010 Elazığ earthquake, which was observed in region H and the second one was 03 November, 2010 Çanakkale (Saros Gulf) earthquake, observed in region D.

The third was the 22 September, 2011 Erzincan earthquake, which was observed around region G and the fourth one was 07 June, 2012 Marmara Ereğlisi (Tekirdağ), which is observed in the vicinity of region A. Thus, anomalies of spatial and temporal variation on seismicity rates where the seismic quiescence is observed can be regarded as indicators of the next earthquake processes in the NAFZ between 2010 and 2012.

## 7. CONCLUSIONS

In this study, a detailed statistical analysis is made to investigate the spatial and temporal variations of seismicity patterns along the North Anatolian Fault Zone. For this pur-

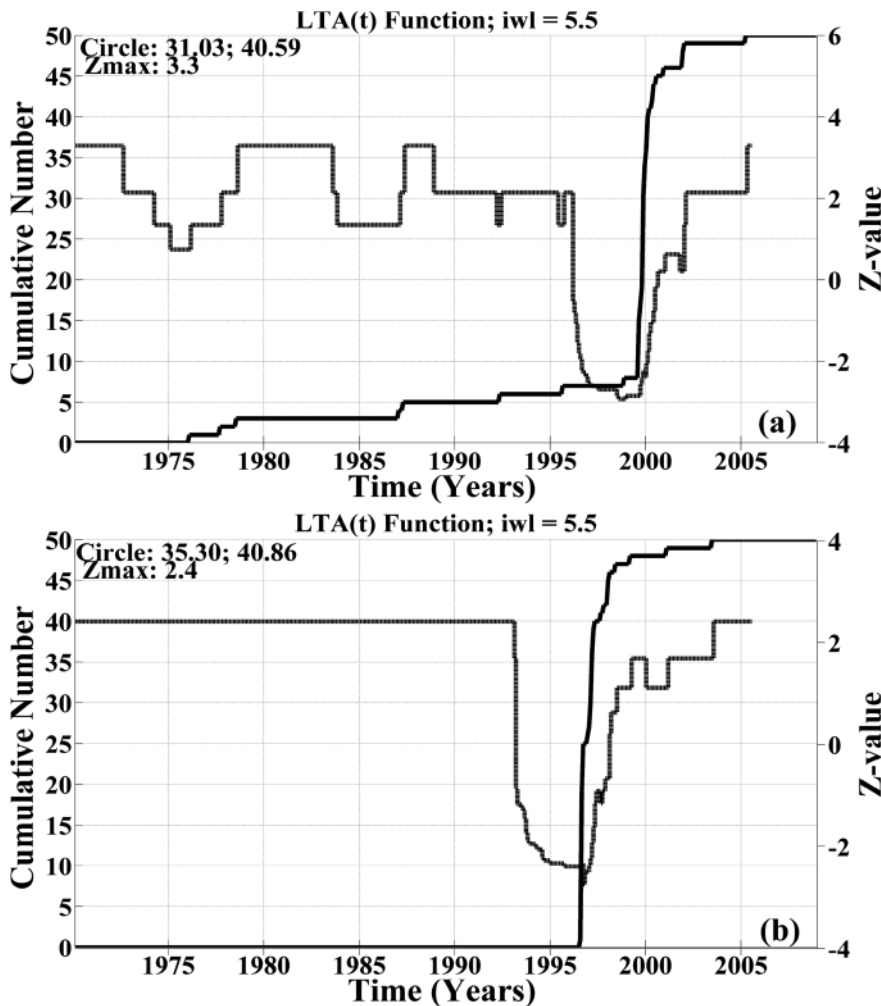


FIGURE 10: Cumulative number and Z-value plots versus time for the anomaly areas detected in the Anatolian part of North Anatolian Fault Zone in Figure 9 for (a) region E, (b) region F.

pose, we focus on the detection of the seismic quiescence situation in the beginning of 2009 at the fault zone. In the analyses, 16,295 crustal earthquakes of magnitude equal and greater than 1.4, with depths less than 70 km are obtained. The final catalogue is complete for whole study period and for all magnitude levels and homogeneous for duration magnitude.

The  $b$ -values for all regions are close to 1 and typical for earthquake catalogues. The Reasenberg algorithm is used to separate the dependent events and the earthquake catalogues for all regions are declustered for Z-value calculations. There are eight regions showing the current seismic quiescence on the North Anatolian Fault Zone in the beginning of 2009. On the Marmara part of the North Anatolian Fault Zone, three anomalies are found centered at 41.08°N-28.58°E (around Silivri), 41.47°N-29.51°E (in the Black Sea), 40.69°N-29.78°E (including Izmit) and 40.26°N-26.46°E (around Çanakkale, Saros Gulf). The other two quiescence areas are found centered at 40.59°N-31.03°E (including Düzce fault) and 40.86°N-35.30°E (around Amasya) on the Anatolian part of the North Anatolian Fault Zone. The rest of the quiescence anomalies are situated at 39.48°N-39.74°E (around Erzincan) and 39.06°N-40.50°E (including Elazığ and Bingöl) on the Eastern part of the North Anatolian Fault Zone. These areas of seismic quiescence recently observed and starting in the beginning of 2005 in eight aforementioned regions can be considered as the most significant.

The last earthquakes “MW=6.0-Elazığ earthquake, 2010 March 08, MW=5.2-Çanakkale (Saros Gulf) earthquake, 2010 November 03, MW=5.5-Erzincan earthquake, 2011 September 22 and MW=5.1- Marmara Ereğlisi (Tekirdağ), 2012 June 07” occurred where the seismic quiescence is observed among the investigated areas and an outstanding

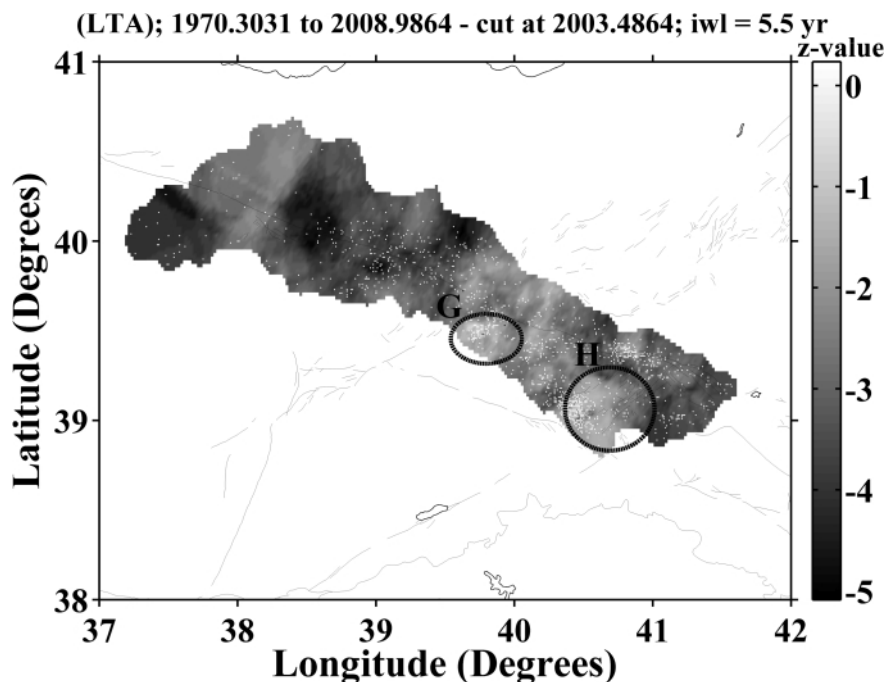


FIGURE 11: Spatial variability of Z-value for the Eastern part of the North Anatolian Fault Zone in the beginning of 2009 with  $T_w$  (iwl)=5.5 years. Calculations are made by using the declustered earthquakes with  $M_p \geq 2.9$  for this region.

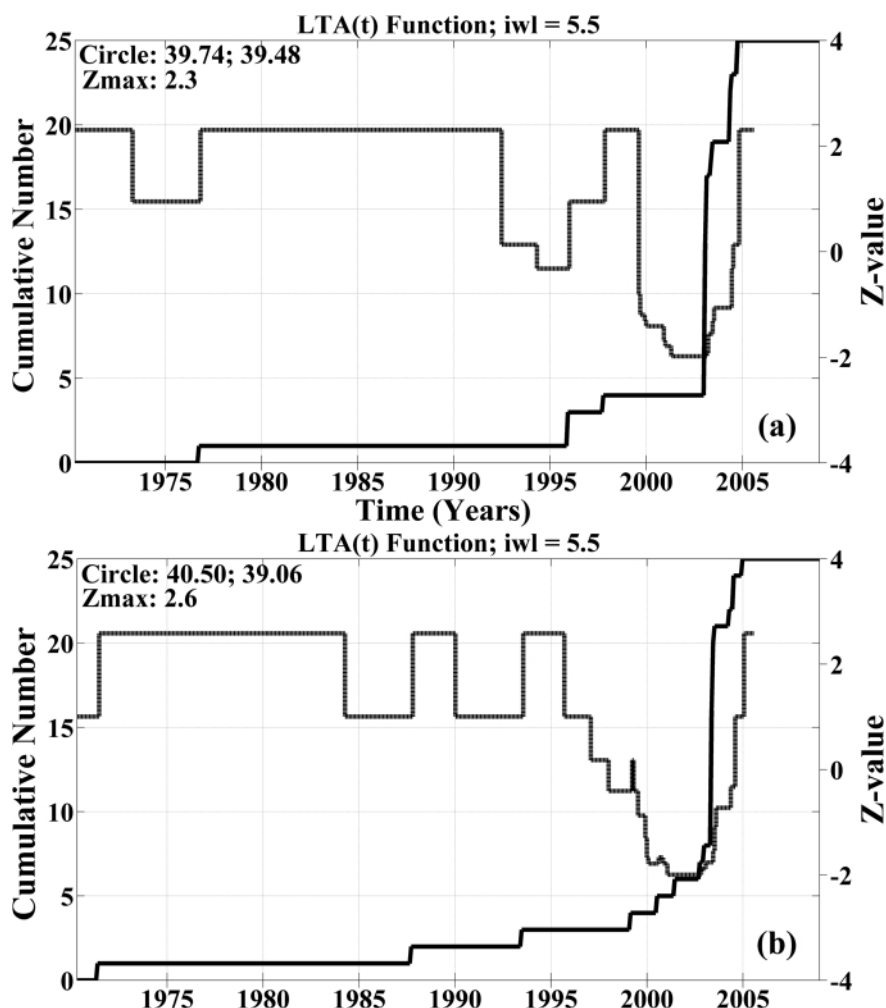


FIGURE 12: Cumulative number and Z-value plots versus time for the anomaly areas detected in the Eastern part of North Anatolian Fault Zone in Figure 11 for (a) region G, (b) region H.

seismic quiescence before these main shocks is observed. For this reason, organizations of such kind of spatial and temporal analysis of seismicity can be inferred as one of the symptomatic seismicity patterns for the "seismic quiescence" phenomenon before strong earthquakes in the NAFZ.

#### ACKNOWLEDGEMENTS

The author would like to thank to Prof. Dr. Stefan Weimer for providing ZMAP software. The author would also like to express his sincere thanks to the editor and anonymous reviewers for their useful and constructive comments and suggestions in improving this paper. I am grateful to Dr. Doğan Kalafat (KOERI) for providing the earthquake catalogue. I also thank to KOERI for providing earthquake database via internet.

#### REFERENCES

- Aki, K., 1965. Maximum likelihood estimate of  $b$  in the formula  $\log N = a - bM$  and its confidence limits. University of Tokyo, Bulletin of the Earthquake Research Institute, 43, 237-239.
- Ambraseys, N.N., 1988. Engineering seismology: Part I. Earthquake Engineering of Structural Dynamics, 17(1), 1-50.
- Arabasz, W.J. and Hill, S.J., 1996. Applying Reasenberg's cluster analysis algorithm to regional earthquake catalogs outside California (abstract). Seismological Research Letters, 67(2), p. 30.
- Bayrak, Y., Öztürk, S., Çinar, H., Kalafat, D., Tsapanos, T.M., Koravos, G.Ch. and Leventakis, G.A., 2009. Estimating Earthquake Hazard Parameters from Instrumental Data for Different Regions in and around Turkey. Engineering Geology, 105, 200-210.
- Bektas, O., Eyuboglu, Y. and Maden, N., 2007. Different modes of stress transfer in a strike-slip fault zone: an example from the North Anatolian Fault System in Turkey. Turkish Journal of Earth Sciences, 16, 1-12.
- Bozkurt, E., 2001. Neotectonics of Turkey-a synthesis. Geodinamica Acta, 14, 3-30.
- Chouliaras, G. and Stavrakakis, G.N., 2001. Current seismic quiescence in Greece: Implications for seismic hazard. Journal of Seismology, 5, 595-608.
- Console, R., Montuori, C. and Murru, M., 2000. Statistical assessment of seismicity patterns in Italy: Are they precursors of subsequent events? Journal of Seismology, 4, 435-449.
- Gentili, S., 2010. Distribution of seismicity before the larger earthquakes in Italy in the time interval 1994-2004. Pure Applied Geophysics, 167, 933-958.
- Gutenberg, R. and Richter, C.F., 1944. Frequency of earthquakes in California. Bulletin of the Seismological Society of America, 34, 185-188.
- Habermann, R.E. and Wyss, M., 1984. Seismic quiescence and earthquake prediction on the Cala-Eras Fault, California. Abstract, EOS Transactions, American Geophysical Union, 65, 988.
- Habermann, R.E., 1988. Precursory seismic quiescence: past, present and future. Pure Applied Geophysics, 126, 279-332.
- Huang, Q., Öncel, A.O. and Sobolev, G.A., 2002. Precursory seismicity changes associated with the  $M_w=7.4$  1999 August 17 Izmit (Turkey) earthquake. Geophysics Journal International, 151(1), 235-242.
- Joswing, M., 2001. Mapping seismic quiescence in California. Bulletin of the Seismological Society of America, 91(1), 64-81.
- Katsumata, K. and Kasahara, M., 1999. Precursory seismic quiescence before the 1994 Kurile Earthquake ( $M_w=8.3$ ) revealed by three independent seismic catalogs. Pure and Applied Geophysics, 155, 43-470.
- Kumazawa, T., Ogata, Y. and Toda, S., 2010. Precursory seismic anomalies and transient crustal deformation prior to the 2008  $M_w=6.9$  Iwate-Miyagi Nairiku, Japan, earthquake. Journal of Geophysical Research, 11, B10312.
- Kutoglu, H.S. and Akcin, H., 2006. Determination of the 30-year creep trend on the Ismetpasa segment of the North Anatolian Fault using an old geodetic network. Earth Planets Space, 58, 937-942.
- Kutoglu, H.S., Akcin, H., Kemalder, H. and Gormus, K.S., 2008. Triggered creep rate on the Ismetpasa segment of the North Anatolian Fault. Natural Hazards and Earth System Sciences, 8, 1369-1373.
- Langridge, R.M., Stenner, H.D., Fumal, T.E., Christofferson, S.A., Rockwell, T.K., Hartleb, R.D., Bachhuber, J. and Barka, A.A., 2002. Geometry, slip distribution, and kinematics of surface rupture on the Sakarya Fault Segment during the 17 August 1999 Izmit, Turkey, earthquake. Bulletin of the Seismological Society of America, 92(1), 107-125.
- Mogi, K., 1969. Some features of recent seismic activity in and near Japan, {2}: Activity before and after great earthquakes. University of Tokyo, Bulletin of the Earthquake Research Institute, 47, 395-417.
- Murru, M., Console, R. and Montuori, C., 1999. Seismic quiescence precursor to the 1983 Nihonkai-Chubu ( $M7.7$ ) earthquake, Japan. Annali Geophysica, 42(5), 871-882.
- Öztürk, S., 2009. An Application of the Earthquake Hazard and Aftershock Probability Evaluation methods to Turkey Earthquakes. PhD Thesis, Karadeniz Technical University, Trabzon, 346 pp.

- Öztürk, S., Bayrak, Y., Çinar, H., Koravos, G.Ch. and Tsapanos, T.M., 2008. A quantitative appraisal of earthquake hazard parameters computed from Gumbel I method for different regions in and around Turkey. *Natural Hazards*, 47, 471-495.
- Polat, O., Gok, E. and Yilmaz, D., 2008. Earthquake hazard of the Aegean extension region (West Turkey). *Turkish Journal of Earth Sciences*, 17, 593-614.
- Reasenber, P.A., 1985. Second-order moment of Central California Seismicity, 1969-1982. *Journal of Geophysical Research*, 90, 5479-5495.
- Reasenber, P.A. and Jones, L.M., 1989. Earthquake hazard after a main shock in California. *Science*, 243, 1173-1176.
- Reilinger, R.E., McClusky, S.C., Oral, M.B., King, W. and Toksöz, M.N., 1997. Global Positioning System measurements of present-day crustal movements in the Arabian-Africa-Eurasia plate collision zone. *Journal of Geophysical Research*, 102, 9983-9999.
- Rudolf-Navaro, A.H., Muñoz-Diosdado, A. and Angulo-Brown, F., 2010. Seismic quiescence patterns as possible precursors of great earthquakes in Mexico. *International Journal of the Physical Sciences*, 5 (6), 651-670.
- Şaroğlu, F., Emre, O. and Kuşcu, I., 1992. Active fault map of Turkey. General Directorate of Mineral Research and Exploration, Ankara, Turkey.
- Turk, T. and Gumusay, U., 2008. Design and application of disaster information system infrastructure on the North Anatolian Fault Zone (NAFZ). *The International Archives of the Photogrammetry, Remote Sensing and Spatial Information Sciences*. Vol. XXXVII. Part B8.
- Wang, J., Liu, W. and Zhang, J., 2010. Seismicity gap and seismic quiescence before 1999 Jiji (Chi-Chi)  $M_w7.6$  earthquake. *Earthquake Science*, 23(4), 325-331.
- Wiemer, S. and Wyss, M., 1994. Seismic quiescence before the Landers ( $M=7.5$ ) and Big Bear (6.5) 1992 earthquakes. *Bulletin of the Seismological Society of America*, 84, 900-916.
- Wiemer, S. and Katsumata, K., 1999. Spatial variability of seismicity parameters in aftershock zones. *Journal of Geophysical Research*, 104(B6), 13135-13151.
- Wiemer, S., 2001. A software package to analyze seismicity: ZMAP. *Seismological Research Letters*, 72(3), 373-382.
- Wu, Y.M. and Chiao, Y.L., 2006. Seismic quiescence before the 1999 Chi-Chi, Taiwan,  $M_w7.6$  Earthquake. *Bulletin of the Seismological Society of America*, 96(1), 321-327.
- Wu, Y.M. and Chen, C.C., 2007. Seismic reversal pattern for the 1999 Chi-Chi, Taiwan,  $M_w7.6$  earthquake. *Tectonophysics*, 429, 125-132.
- Wyss, M., 1986. Seismic quiescence precursors to the 1983 Kōiki ( $M_s=6.6$ ), Hawaii earthquake. *Bulletin of the Seismological Society of America*, 76, 785-800.
- Wyss, M., 1997a. Second round of evaluations of proposed earthquake precursors. *Pure and Applied Geophysics*, 149(1), 3-16.
- Wyss, M., 1997b. Case 23 nomination of seismic quiescence as a significant precursor. *Pure and Applied Geophysics*, 149 (1): 79-113.
- Wyss, M. and Burford, R.O., 1987. Occurrences of predicted earthquake on the San Andreas fault. *Nature*, 329, 323-325.
- Wyss, M., Habermann, R.E. and Griesser, J.C., 1984. Seismic quiescence and asperities in the Tonga-Kermadec Arc. *Journal of Geophysical Research*, 89, 9293-9304.
- Wyss, M., Shimazaki, K. and Urabe, T., 1996. Quantitative mapping of a precursory quiescence to the Izu-Oshima 1990 ( $M=6.5$ ) Earthquake, Japan. *Geophysical Journal International*, 127, 735-743.
- Wyss, M. and Martirosyan, A.H., 1998. Seismic quiescence before the  $M7$ , 1988, Spitak earthquake, Armenia. *Geophysical Journal International*, 134, 329-340.

Received: 17 September 2012

Accepted: 13 November 2013

Serkan ÖZTÜRK

Gümüşhane University, Department of Geophysics, TR-29100, Gümüşhane, Turkey;  
serkanozturk@gumushane.edu.tr